A&A 415, 731–737 (2004)
DOI: 10.1051/0004-6361:20034430

Astronomy & Astrophysics

Two-dimensional spectroscopy of a sunspot

II. Penumbral line asymmetries

R. Schlichenmaier, L. R. Bellot Rubio, and A. Tritschler

Kiepenheuer–Institut für Sonnenphysik, Schöneckstr. 6, 79104 Freiburg, Germany

Received 2 October 2003 / Accepted 13 November 2003

Abstract. We present, analyse, and interpret line asymmetries from Fe I 557.6 nm of a sunspot penumbra at a heliocentric angle of 23° with high spatial (0.5 arcsec) and spectral ($\lambda/\triangle\lambda$ = 250 000) resolution. The data set is described and presented in the first paper of this series (Tritschler et al. 2004). Line bisectors are used to quantify the line asymmetries. Our findings are: (1) For averaged limb and center side bisectors the shift increases linearly with the bisector intensity level, but the limb side bisector is more inclined than the center side bisector. (2) Individual bisectors exhibit kinks, such that the bisector at high intensity levels is shifted towards the red for both, limb and center side bisectors. Some of the kinks produce bisector reversals in the outer center side penumbra. The bisector properties and their intriguing differences between center and limb side can be explained if one assumes downflows in deep atmospheric layers ($\log\tau > -1$). This is demonstrated by synthetic bisectors. The differences between the two penumbral sides are due to projection effects of non-horizontal flow channels. Our findings also imply that bisectors reversals are not due to elevated channels, but due to the presence of downflows. Along a specific center side flow filament the bisector shift is found to be largest in the line wing, except for the outer end of the filament, where a kink at high bisector intensities toward the red is found. This is consistent with an upflow at the inner footpoint, a deep lying horizontal flow, and, after a spatial distance of 4 arcsec, with a downflow at the end of the flow filament.

Key words. Sun: activity – Sun: photosphere – Sun: sunspots – techniques: spectroscopic – line: formation

1. Introduction

A conspicuous feature in the photosphere of a sunspot penumbra is the Evershed effect, which consists of a line shift, and a line asymmetry (Bumba 1960; Servajean 1961) in photospheric absorption lines (for reviews see, e.g., Schröter 1967; Maltby 1997; Wiehr 1999; Schlichenmaier 2003). The degree of line shift and line asymmetry depends on the strength of the absorption line. To be exact, it depends on the formation height of the line: deep forming, weak lines show relatively strong line core shifts (red-shifts on limb side penumbra and blue-shifts on center side penumbra) and no significant line asymmetry, i.e., the line is shifted "as a whole". Lines whose cores form in higher, but still photospheric, atmospheric layers (and which are typically stronger) only show relatively small line core shifts, while the wings are more shifted than the line core, namely to the red on the limb side penumbra and to the blue on the center side penumbra (e.g., Stellmacher & Wiehr 1971, 1980; Wiehr et al. 1984; Ichimoto 1987, 1988).

Today, it is common wisdom that penumbral line shifts and asymmetries are to be interpreted as mass flows rather than as surface waves (Thomas 1994; Bünte & Solanki 1995). From the dependence of the blue-shifts in the center side penumbra and red-shifts in the limb side penumbra on the heliocentric angle, it can be concluded that the flow is a radial outflow, which is predominantly horizontal. In recent years evidence has accumulated that vertical flow components are also present which potentially solve the problem of mass conservation of the Evershed flow (Rimmele 1995; Westendorp Plaza et al. 1997; Schlichenmaier & Schmidt 2000; Schmidt & Schlichenmaier 2000; Westendorp Plaza et al. 2001a,b; del Toro Iniesta et al. 2001; Bellot Rubio et al. 2003a). In particular, downflows in deep photospheric layers of the outer penumbra have been detected, which at least qualitatively explain the abrupt stop of the Evershed flow at the outer penumbral boundary.

Line bisectors are used to investigate the line asymmetry: at a certain intensity level, the line bisector measures the mean Doppler shift of the two intersection points with the line profile. Non-vertical bisectors, i.e., asymmetric lines, can in principle be interpreted as a superposition of two or more flow components (1) that are spatially unresolved within the resolution elements or/and (2) that are not resolved in depth, due to the fact that the contribution functions cover extended height ranges in the atmosphere. As a rule of thumb, it can be said that the line wing is formed in deep layers while the line core is formed higher up. Maltby (1964) realized that the observed line asymmetries could be explained by a velocity configuration in

Send offprint requests to: R. Schlichenmaier,
e-mail: schliche@kis.uni-freiburg.de

which flows are only present in the deepest photospheric layers ($\log\tau > -1$).

Controversial findings on the shape of the bisector have been presented. Holmes (1963), Maltby (1964), Hirzberger & Kneer (2001), and Balasubramaniam (2002) find that the bisector shift increases monotonically with increasing intensity, while Schröter (1965), Wiehr et al. (1984), and Rimmele (1995) find that the bisector shift exhibits an extremum at intermediated intensity levels, i.e. a bisector reversal. The latter finding is consistent with results from Westendorp Plaza et al. (2001b) who reconstructed the line-of-sight[1] velocity variation with height by inverting spectropolarimetric data. Yet, it is not controversial that the shape of the bisector is different for the limb side and the center side penumbra (Schröter 1965; Rimmele 1995; Westendorp Plaza et al. 2001b; Balasubramaniam 2002). Rimmele and Westendorp Plaza et al. interpreted the presence of a bisector reversal as being due to elevated flow channels and the difference between the bisector shapes of limb and center side penumbra as being due to differential opacity effects. They propose that different geometrical heights are seen at equal optical depths in the limb and center side penumbra. Curiously enough, one of them claimed that deeper layers are observed on the limb side, while the other inferred that deeper layers are observed on the center side penumbra.

The mentioned findings and claims, which are inconsistent in some respects, are the motivation for this work, which is the second paper of a series on the data set which we presented in Paper I (Tritschler et al. 2004). In Sect. 2 we describe our measurements. We investigate the shapes of bisectors (Sect. 3), and show in Sect. 4 that the shapes of the bisectors can be explained if one assumes downflows in deep photospheric layers. On this basis, we present a flow configuration which is capable of qualitatively reproducing the different bisector shapes on the center and limb sides of the penumbra. In our interpretation differential opacity effects are not needed, and the flow is concentrated in the deep photosphere. We summarize our conclusions in Sect. 5.

2. Observations

We analyse and interpret the line asymmetries of a 2-dimensional data set at high spatial (≈0.5 arcsec) and spectral ($\lambda/\triangle\lambda \approx 250\,000$) resolution. The data set was acquired with TESOS (Triple Etalon Solar Spectrometer) at the VTT in Izaña (Tenerife), taking advantage of the Kiepenheuer-Institute Adaptive Optics System (KAOS). The measurements are performed in the neutral iron line at 557.6 nm. This line probes the layers between the continuum forming layers up to a optical depth of $\log\tau \approx -3$. It is insensitive to magnetic fields ($g = 0$) and is therefore ideally suited to study the photospheric velocity fields. The spot under investigation is located at a heliocentric angle of 23°. More details on the data acquisition, reduction, and the velocity calibration are described in Tritschler et al. (2004).

[1] Hereafter, line-of-sight is abbreviated by LOS.

3. Bisector shapes of Fe I 557.6 nm

3.1. Observed bisector shapes and their dependence on the location within the penumbra

We construct bisectors for each line profile of the two-dimensional map. The bisector is constructed by measuring the Doppler shifts at 40 intensity levels of the line with a spacing of 2%. The intensity difference between the line core and the local continuum corresponds to 100%, i.e. we study the bisector for intensity levels between 2% and 80%. For higher intensity levels the bisector becomes unreliable, since the bisector positions are very sensitive to noise once the continuum of the line is approached.

In Fig. 1 we present a sample of penumbral bisectors. The array of bisectors corresponds to the marked white squares which are overplotted in the sunspot continuum image to the right. The upper half (#1 through #24) corresponds to the limb side penumbra, and the lower half (#25 through #48) to the center side penumbra. The plotted bisectors are retrieved from the line profile being averaged over the corresponding white squares. They contain 4×4 profiles and have a size of 0.4×0.4 arcsec^2, which is slightly smaller than the spatial resolution of our data set. The bisectors from the black squares reflect mean bisectors of larger areas (3.8×3.8 arcsec^2) from the limb side (upper right) and center side (lower right) penumbra.

The behaviour of the mean bisectors (black squares) can be described as follows: At the 2% intensity level, i.e. at the line core, the two bisectors exhibit a small blue-shifted velocity of some hundred m s^{-1}. The bisector shift increases towards the wing, to the red on the limb side and to the blue on the center side. In both cases, the shift increases linearly with intensity. However, the two bisectors differ in their slope, with the limb side bisector being more inclined than the center side bisector, leading to a red-shift of 1.3 km s^{-1} on the limb side and a blue-shift of only about -1 km s^{-1} on the center side at the 80% intensity level.

The individual bisectors (white squares) follow the general trend of the mean bisectors (black squares), but depending on their location they deviate from the described properties by exhibiting kinks:

1. Some of the center side bisectors (e.g., #38, #41 to #48, marked with little arrows in Fig. 1) have the tendency that the shift increases less than linearly towards the higher intensity levels, i.e. they exhibit a kink towards the red;
2. The shift of limb side bisectors tend to increase more than linearly (e.g., #5 to #8, #11, #12, #15 to #18), i.e. they also exhibit a kink towards the red;
3. In the very outer center side penumbra (bottom row in Fig. 1), the shift of some bisectors even decreases for high intensity levels, i.e. these bisectors do not only show a kink, but a reversal.

Our finding that the slopes of the bisectors differ between limb and center side penumbra is consistent with previous findings of Schröter (1967), Rimmele (1995), and Westendorp Plaza et al. (2001b, although they do not show bisectors in their Fig. 4, but the velocity dependence on optical depth). However,

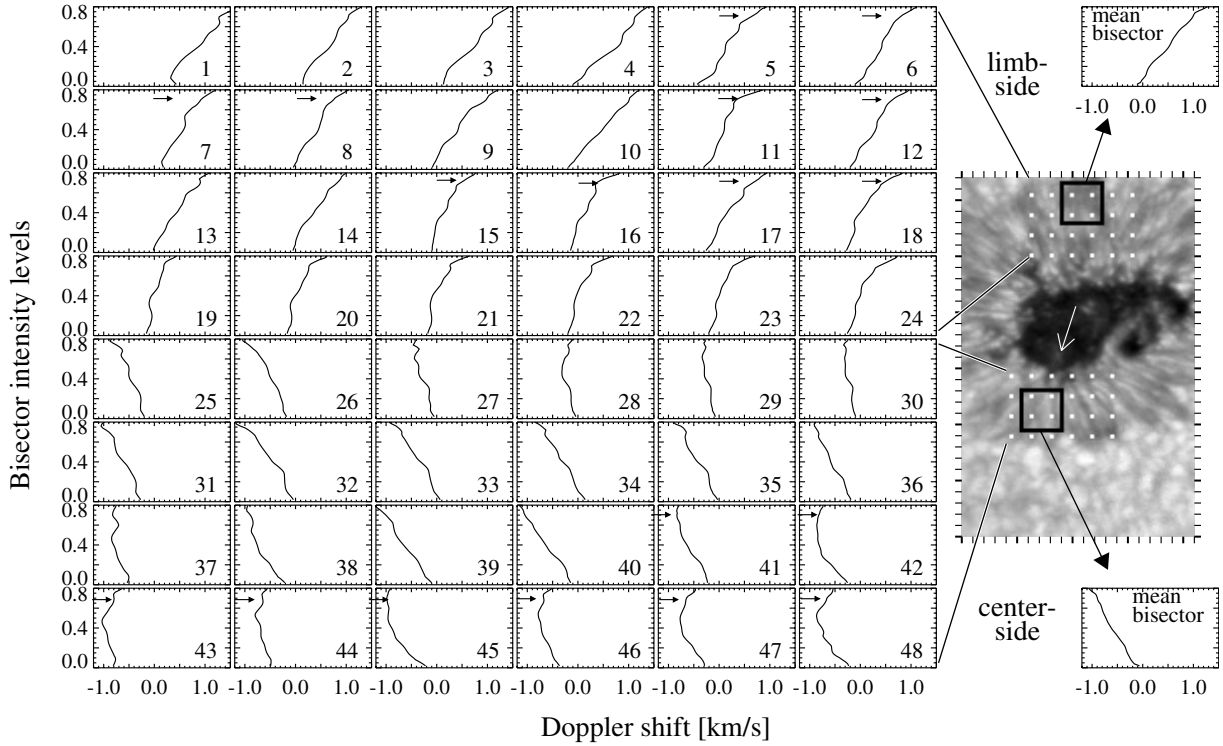

Fig. 1. Bisectors of Fe I 557.6 nm. We plot an array of bisectors for the limb side and center side penumbra which corresponds to the spatial averages of the small white squares in the image to the right. The intensity level is normalized relative to the line profile between the continuum and the line core level. The bisectors are shown for intensity levels between 2% and 80%. The bisector shift from the reference wavelength is converted into Doppler velocity in units of km s^{-1}. The upper and lower right bisectors (above and beneath the sunspot image) stem from the spatially averaged line profiles (marked with the black squares in the sunspot image) from the limb and center side, respectively. The white arrow in the umbra points towards disk center. The tickmarks in the image correspond to 1 arcsec.

in contrast to the first two authors we (and the latter authors) do not find bisector reversals on the limb side penumbra. Instead we find that bisector reversals are only present in the very outer center side penumbra. We note that Holmes (1963), Maltby (1964), and Hirzberger & Kneer (2001) do not find evidence for bisector reversals.

3.2. Bisectors in and around a flow filament

Before discussing possible explanations of the differences between the limb and center side penumbra, we concentrate on bisectors in and around an individual filament. The filament that we choose is one of the center side flow filaments that we also discussed in Sect. 5.5.1 of Paper I. In Fig. 2 we show a blow-up of the line wing Doppler map computed for bisector intensities between 60% and 80% (left image) and a continuum intensity map (right image). We present bisectors along the flow filament (middle column) and from the surroundings of the filament (left and right column). The line wing blue-shift along the filament increases from -1.2 km s^{-1} at bisector #2 to reach a maximum of some -1.5 km s^{-1} at bisector #8, and then decreases in bisector #11 to -1.0 km s^{-1}. While #2, #5, and #8 are roughly linear, bisector #11 exhibits a kink (marked with a little arrow), which is typical for the outer center side penumbra. In the next section, we interpret the presence of the kink as being due to downflows in the deep photosphere.

The bisectors adjacent to the flow filament (left and right column) also show strong line wing blue-shifts, although these shifts are smaller than within the flow filament. This might be interpreted such that the flow is only enhanced within the flow filament, but present also in its surroundings. Then the common concept of flow channels, which tacitly assumes a background of the flow channel at rest, seems erroneous. However, it may also be that the presence of a flow outside the flow filament is due to the fact that we do not spatially resolve the individual flow channels. Since we cannot settle this question from our data set, we prefer to use the notion of "flow filaments" instead of "flow channels".

4. Interpretation of bisector shapes

In this and the next section we aim at an understanding of the observed bisector shapes, especially on their different behaviour on limb and center side.

We first concentrate on the averaged limb side bisector (upper black squares in Fig. 1). The mere fact that their Doppler shift increases with increasing intensity level indicates that the Evershed flow resides in deep photospheric layers, i.e., close to the continuum forming layer (Maltby 1964; Schlichenmaier 1999, 2003). We note that others have alternatively interpreted the shape of the bisectors as a velocity gradient along the LOS (e.g., Stellmacher & Wiehr 1980), but here we adhere to the idea of Maltby who demonstrates that a velocity discontinuity

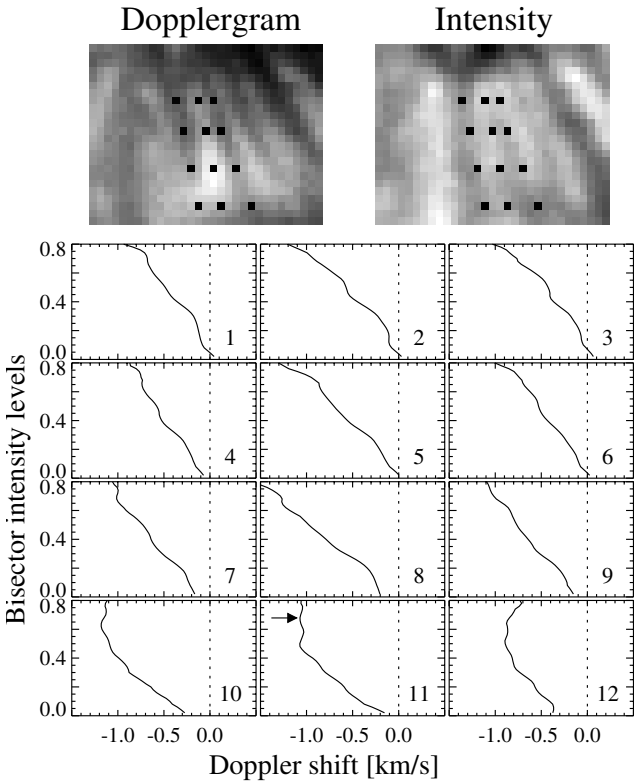

Fig. 2. Bisectors in and around a flow filament: a zoomed-in line wing Doppler map (from bisector intensities between 60% and 80%) is shown in the upper left image for a portion of the center side penumbra (5.4×4.0 arcsec^2). The upper right image displays the corresponding continuum intensity map. Along and adjacent to one individual flow filament we display the bisectors, which correspond to the black squares within the images. The squares and the displayed bisectors correspond to 0.2×0.2 arcsec^2.

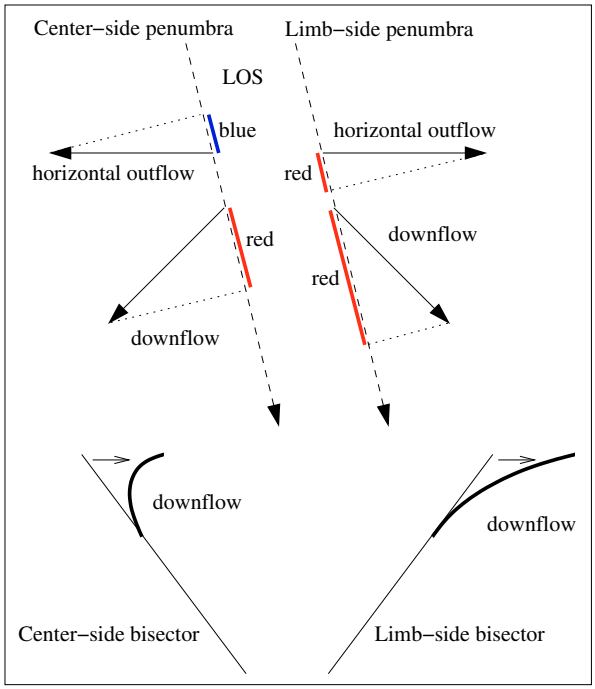

Fig. 3. Sketch illustrating how downflows influence the shape of the bisector. On the center side the bisectors are blue-shifted by the Evershed flow. A deep-lying downflow adds a red-shift (at high intensity levels) to the blue-shifted bisector, leading to a reversal (left panel) or at least to a bisector "kink towards the red". On the limb side the bisectors are red-shifted by the Evershed flow. A deep-lying downflow adds a red-shift (at high intensity levels), leading to a "kink" towards higher red-shifts in the bisector.

along the LOS and flow channels in the deepest photospheric layers are able to reproduce qualitatively the observed shapes of the bisectors. On the center side penumbra, the averaged bisector (lower black square in Fig. 1), although less inclined, shows the same behaviour as on the limb side penumbra, i.e. indicating a deep-lying Evershed flow as well.

As we will demonstrate in Sect. 4.1.1, the different slopes of the mean bisectors can be obtained by following Malby's idea and assuming a mean downward component of the flow: then, the LOS velocity is larger on the limb side, and larger shifts result on the limb side as compared to the center side. However, the challenge is not only to explain the different slopes of the mean bisector, but also the fact that some bisectors show kinks and reversals, predominantly in the outer penumbra.

Rimmele interpreted such bisector reversal in terms of elevated flow channels: the largest Doppler shift occurs in the mid-photosphere (medium bisector intensity), while the upper photosphere (low bisector intensity) and the deep photosphere (high bisector intensity) are essentially unshifted. In agreement with Westendorp Plaza et al. (2001b) he put forward differential opacity effects to explain the differences between limb and center side penumbrae, meaning that different geometrical layers are viewed on the two penumbral sides. However, the two articles do not agree on the question on which side deeper layers are viewed. We believe that such differential opacity effects cannot be large, and note that the influence of downflows on the bisector shape has so far not been investigated. As we will demonstrate below, downflows can reproduce the observations.

To explain the individual bisectors of the outer penumbra that show the mentioned properties, it is not sufficient to have only one inclination of the flow along the LOS. Therefore instead of assuming only one flow inclination along the LOS as we did to obtain the mean bisectors, we assume two flow inclinations along the LOS of the flow component: an essentially horizontal flow at an optical depth around $\log \tau = -1$ together with a downflow component in deeper continuum forming layers. For the angle of the downflow we use a downward inclination of 45° with respect to the horizontal. The scenario we have in mind is illustrated in Fig. 3:

- On the limb side the downflow component being located in the very deep photosphere would add to the red-shift of the horizontal flow component, leading to an additional red-shift at high bisector levels;
- On the center side, the horizontal flow component causes a blue-shifted bisector. However, the deep-lying highly inclined downflow component is red-shifted (at sufficiently small heliocentric angles). Then the high intensity bisector levels would experience a red-shift, leading to the observed

reversal of the bisector, or at least to a "less-than-linear" increase of bisector shift with increasing intensity levels.

4.1. Forward modelling of bisectors

In order to check whether or not the scenario we propose in the previous section is feasible, we calculate synthetic lines and their bisectors to reproduce qualitatively the observed bisector shapes. Several assumption on the line formation have to be made:

1. The temperature and pressure stratification must be given. We use the mean penumbral model atmosphere that was obtained by inverting the profiles of the same data set (Bellot Rubio et al. 2003b). This atmosphere is essentially the same as the ones published by del Toro Iniesta et al. (1994) and Rouppe van der Voort (2002);
2. For the macro-turbulence, micro-turbulence and spectral resolution we assume values of 1 $\mathrm{km\,s^{-1}}$ ($\hat{=}$1.9 pm), 1.5 $\mathrm{km\,s^{-1}}$ ($\hat{=}$2.8 pm), and 2.2 pm, respectively;
3. We assume that two components (see discussion below) are present within the resolution element:
   (a) One background component at rest, which represents a magnetic field component that is inclined with respect to the horizontal;
   (b) and another component with a filling factor of 50% in which flows reside along the LOS.
4. Motivated by simulations of magnetic flux tubes within the penumbra (e.g., Schlichenmaier 2002), we assume that the flows have a velocity of 8 $\mathrm{km\,s^{-1}}$;
5. In all calculations we assume a heliocentric angle of 23°.

The assumption of two components (third point of the upper list) reflects that the flow component cannot fill the entire volume. Some fraction of the volume (we assume 50%) is filled with the overall magnetic field component that is known to be inclined with respect to the horizontal. This *background* component is assumed to be at rest. Within the flow component, flow channels that are embedded in an atmosphere at rest are present. This configuration represents the concept of the uncombed penumbra (Solanki & Montavon 1993; Martínez Pillet 2000; Müller et al. 2002) and takes into account that the magnetic fields, which are inclined with respect to the horizontal, have to penetrate all layers. The described configuration is consistent with assumptions and conclusions in Schlichenmaier (2002), Bellot Rubio et al. (2003a), and Schlichenmaier & Solanki (2003).

4.1.1. Different bisector slopes

To explain the different slopes of the mean bisectors, we follow the model of Maltby (1964) and additionally assume that the mean flow is slightly inclined downwards. For the line synthesis the flow channel along the LOS is placed at $-1.0 < \log\tau < 0.5$, with an absolute velocity of 8 $\mathrm{km\,s^{-1}}$ and an inclination of 95° with respect to the vertical, i.e., 5° relative to the horizontal. Due to projection effects the LOS velocity on the limb side (upper left panel of Fig. 4) is larger than the corresponding LOS velocity on the center side (lower left panel of Fig. 4).

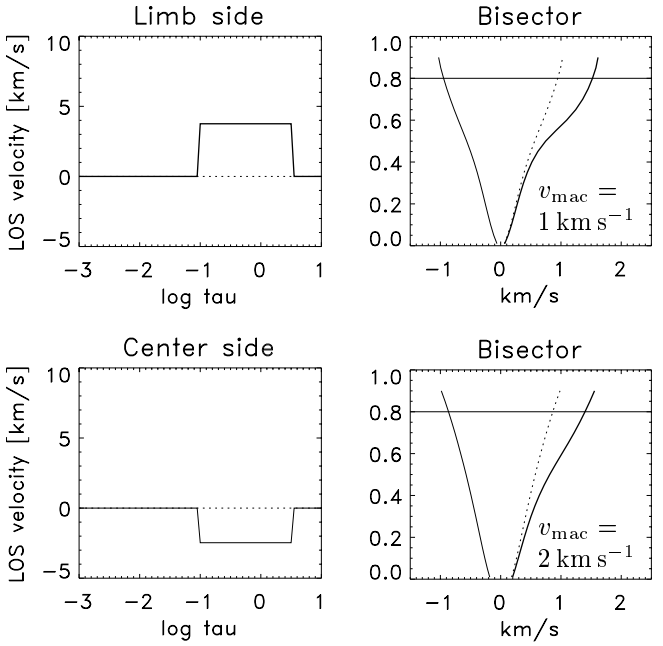

Fig. 4. Synthetic bisectors with different slopes: the upper and lower left panel show the LOS velocities of a flow channel in the deep photosphere for the limb and center side, respectively. The flow has an absolute velocity of 8 $\mathrm{km\,s^{-1}}$ and a downward angle with respect to the horizontal of 5°. The solid line traces the flow component, while the dotted line reflects the background component at rest. The right panels show the corresponding synthetic bisectors for a macro-turbulence of 1 $\mathrm{km\,s^{-1}}$ (top) and 2 $\mathrm{km\,s^{-1}}$ (bottom). The red-shifted (thick) solid lines correspond to the limb side bisectors and the blue shifted (thin) solid lines correspond the the center side bisector. For better comparison with the limb side bisector, the dotted line represents a reflection of the center side bisector.

The upper right panel of Fig. 4 displays the two corresponding bisectors for a macro-turbulence $v_{\mathrm{mac}} = 1\ \mathrm{km\,s^{-1}}$. The thick line represents the red-shifted limb side bisector, and the thin line represents the blue-shifted center side bisector. For better comparison of the different slopes, the dotted line shows the reflected center side bisector. The lower right panel of Fig. 4 shows the bisectors with a macro-turbulence of 2 $\mathrm{km\,s^{-1}}$.

The fact that a deep-lying flow is not seen as a line satellite, but instead as a more or less smooth inclined bisector is due to all the effects that smear out a clear one-to-one correspondence between the geometrical height in the atmosphere and the intensity level in the line profile. E.g., a small LOS component of the velocity compared to the thermal width of the line, the fact that the line depression contribution function for each intensity level probe a wide range of geometrical heights, the presence of micro and macro-turbulence, and the finite spectral resolution. These smearing effects are apparent, if one compares the bisectors obtained using a macro-turbulence of 1 $\mathrm{km\,s^{-1}}$ (upper right panel of Fig. 4) with those using 2 $\mathrm{km\,s^{-1}}$ (lower right panel of Fig. 4). It is seen that these bisectors are very close to being linear, and reproduce qualitatively the observed mean bisectors (black squares of Fig. 1), which sample the mid and outer penumbra. In these parts of the penumbra downflow

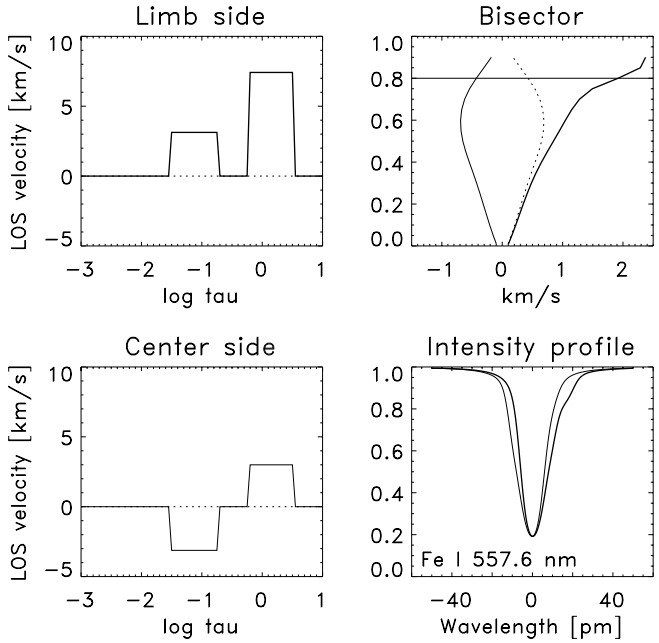

Fig. 5. Synthetic bisector exhibiting kinks: for a flow configuration described in the text, the left panels displayes the velocity component along the LOS for the limb (top) and center side (bottom). The right panel displays the corresponding synthetic bisectors (top), and the line profiles (bottom). Thick solid, thin solid, and dotted lines as in Fig. 4.

components have been found (see Sect. 1 and Paper I), justifying our assumption of a mean flow with an inclination of 95°.

4.1.2. Bisector reversals and bisector kinks

While it is sufficient to use one inclined flow component to reproduce the mean bisectors, two different flow inclinations along the LOS must be assumed to explain the kinks and reversals of individual bisectors in the outer penumbra: Within the flow component, we place one horizontal flow channel in the optical depth range in $\log \tau$ from -1.5 to -0.8, and one inclined flow channel from -0.2 to 0.5. The latter is inclined downward by 45° with respect to the horizontal. In the left panel of Fig. 5 the resulting LOS velocity stratifications at a heliocentric angle of 23° are displayed for the limb (top) and center (bottom) side penumbra.

The resulting line profiles of Fe I 557.6 nm are displayed in the lower right panel of Fig. 5 for the limb side penumbra (thick line) and the center side penumbra (thin line). The corresponding bisectors are shown in the upper right panel of this figure. For better comparison the dotted line shows the reflected center side bisector. The synthetic center side bisector exhibits a reversal, while the synthetic limb side bisector exhibits a kink at some 70%, with shifts that increase more-than-linear with increasing intensities. These results demonstrate that the different shapes of the bisectors can be due to the presence of a downflow component in the very deep photospheric layers, which lead to different projections of the LOS velocity on center and limb side, respectively. We note that this more complex configuration also reproduces the different slopes of center and limb side bisectors.

In other words, the synthetic bisectors that we present in this and the preceeding sections give evidence for the presence of downflows in the outer penumbra. This evidence relies on the shape of bisectors rather than on the calibration of the velocity. As discussed in Paper I the finding of a downflow component in the outer penumbra from the variation of the LOS velocity along azimuthal slices critically depends on the calibration of the velocity. Here we confirm the presence of downflows by interpreting the shape of bisectors.

The bisector shapes along the flow filament of Fig. 2 can be interpreted in the following manner: in the inner part of the filament the bisector at high intensity levels exhibits a kink towards the blue indicating a deep lying blue-shifted flow component. Whether this flow component is essentially horizontal or whether it has an upward component cannot be determined, since only the LOS component of the velocity is measured. In the outer part of the flow filament the bisector exhibits a kink to the red, and we interpret this kink as a downflow component in the continuum forming layers. Hence, we believe that the source of the flow is at the inner end of the filament. The flow continues outwards in the deep photosphere being essentially horizontal. After some 4 arcsec (at the outer end of the filament where we measure the kink in the bisector) the flow dives beneath the visible layers. Such a scenario is consistent with numerical simulations (Schlichenmaier et al. 1998; Jahn et al. 1996; Schlichenmaier 2002) and with estimates on the penumbral heat transport (Schlichenmaier & Solanki 2003).

5. Conclusion

Penumbral line profiles have been studied extensively during the last decades. It was found that profiles from the limb side penumbra have different shifts and asymmetries than profiles from the center side. This difference was thought to be due to a differential opacity effect (Rimmele 1995; Westendorp Plaza et al. 2001b), according to which different geometrical layers are viewed on the two sides. However, inconsistent opinions exist on which side deeper layer are seen. Investigating the bisectors of line profiles, some authors presented evidence that the bisectors exhibit reversals or kinks while others rather find a continuous increase of the bisector shift with the bisector intensity level towards the red on the limb side and towards the blue on the center side. Rimmele (1995) found evidence for bisector reversals also on the limb side and interpreted them as being due to elevated flow channels.

In this work, we investigate the shape of penumbral bisectors of Fe I 556.7 nm with high spatial and high spectral resolution and, confirming previous work, we find intriguing differences between limb side and center side bisectors. Limb side bisectors have a larger tilt than center side bisectors. For profiles averaged on the limb and on the center side, the bisector has a linear shape, i.e., the shift increases linearly with bisector intensity, but with the limb side bisector being more inclined than the center side bisector. We also find bisector reversals, but only in the very outer center side penumbra. There, bisectors have the tendency to show a kink towards the red at high

intensity levels, which sometimes is so strong that the bisector exhibits a reversal. However, on the limb side although we also observe a kink, it is not toward vanishing Doppler shifts, but towards larger redshift at high bisector intensities, consistent with the findings of Westendorp Plaza et al. (2001b). This behaviour cannot be explained by elevated flow channels, if one does not rely on differential opacity effects.

To explain the different slopes of spatially averaged bisectors from the limb and center side penumbra, we propose that the averaged flow field can be described by a flow channel in the deep photosphere (beneath $\log\tau = -1$) that is inclined downwards by 5° with respect to the horizontal. The different bisector slopes are simply due to a projection effect. In order to reproduce kinks and reversals of individual bisectors in the outer penumbra, two different inclination angles along the LOS must be present: one essentially horizontal flow channel around $\log\tau = -1$, and one downflow component in the continuum forming layers. For the downflow we assume an inclination angle of 45° with respect to the horizontal. This flow configuration produces a bisector reversal when viewed on the center side penumbra, and a bisector kink towards the red on the limb side penumbra.

In our synthetic model configuration we assume that the flow is not spatially resolved. Therefore we base our synthetic profiles on two components: a flow component which harbours the flow channels, and another component at rest with a filling factor of 50%. The latter component at rest mimics the background magnetic field which is inclined with respect to the horizontal. It is interesting to realize that absolute flow velocities as high as 8 $\mathrm{km\,s^{-1}}$ are necessary to reproduce bisector shifts of some 1.5 $\mathrm{km\,s^{-1}}$. Such high velocities are predicted by numerical simulations of the moving tube model (Schlichenmaier 2002).

Hitherto, only the azimuthally averaged inclination of the flow could be inferred by assuming an axial symmetric flow field, and such inclination angles critically depend on the proper calibration of the velocity. We demonstrate that the presence of downflows can also be inferred from the finding that the limb and center side bisectors have different slopes.

The spatial resolution of our data is rather high (0.5 arcsec), but still not sufficient to resolve the intrinsic scale of the penumbral flow field. Therefore it is necessary to perform spectroscopic measurements at the resolution limit of large solar telescopes.

Acknowledgements. We gratefully acknowledge the Kiepenheuer adaptive optics system (KAOS) which was essential to acquire our data set. The KAOS team includes D. Soltau, Th. Berkefeld, and Th. Schelenz. We thank Th. Berkefeld for operating KAOS during our observation. Also, we are sincerely grateful to Th. Kentischer, who built, upgraded, programmed, and aligned TESOS and who supported our observations technically. We thank O. Steiner for fruitful discussions. W. Schmidt and C. Denker gave valuable comments on the manuscript. Part of this work was supported by the DFG grants PE 782/4 and Schl 514/2-1.

References

Balasubramaniam, K. S. 2002, ApJ, 575, 553
Bellot Rubio, L., Balthasar, H., Collados, M., & Schlichenmaier, R. 2003a, A&A, 403, L47
Bellot Rubio, L., Schlichenmaier, R., & Tritschler, A. 2003b, A&A, in preparation
Bumba, V. 1960, Izv. Krymk. Astrofiz. Observ., 23, 253
Bünte, M., & Solanki, S. K. 1995, A&A, 297, 861
del Toro Iniesta, J. C., Bellot Rubio, L. R., & Collados, M. 2001, ApJ, 549, L139
del Toro Iniesta, J. C., Tarbell, T. D., & Ruiz Cobo, B. 1994, ApJ, 436, 400
Hirzberger, J., & Kneer, F. 2001, A&A, 378, 1078
Holmes, J. 1963, MNRAS, 126, 155
Ichimoto, K. 1987, PASJ, 39, 329
Ichimoto, K. 1988, PASJ, 40, 103
Jahn, K., Schlichenmaier, R., & Schmidt, H. U. 1996, Astr. Lett. Comm., 34, 59
Müller, D. A. N., Schlichenmaier, R., Steiner, O., & Stix, M. 2002, A&A, 393, 305
Maltby, P. 1964, Astrophys. Norv., 8, 205
Maltby, P. 1997, in 1st Advances in Solar Physics Euroconference. Advances in Physics of Sunspots, ed. B. Schmieder, J. C. del Toro Iniesta, & M. Vazquez, ASP Conf. Ser., 118, 91
Martínez Pillet, V. 2000, A&A, 361, 734
Rimmele, T. R. 1995, A&A, 298, 260
Rouppe van der Voort, L. H. M. 2002, A&A, 389, 1020
Schlichenmaier, R. 1999, in High Resolution Solar Physics: Theory, Observations, and Techniques, ed. T. R. Rimmele, K. S. Balasubramaniam, & R. R. Radick, ASP Conf. Ser., 183, 91
Schlichenmaier, R. 2002, AN, 323, 303
Schlichenmaier, R. 2003, in Current theoretical models and future high resolution solar observations, ed. A. Pevtsov, & H. Uitenbroek, ASP Conf. Ser., 286, 211
Schlichenmaier, R., Jahn, K., & Schmidt, H. U. 1998, A&A, 337, 897
Schlichenmaier, R., & Schmidt, W. 2000, A&A, 358, 1122
Schlichenmaier, R., & Solanki, S. K. 2003, A&A, 411, 257
Schmidt, W., & Schlichenmaier, R. 2000, A&A, 364, 829
Schröter, E. H. 1965, Z. Astrophys., 62, 228
Schröter, E. H. 1967, in Solar Phys., ed. J. N. Xanthakis (London: John Wiley & Sons), 325
Servajean, R. 1961, Ann. Astrophys., 24, 1
Solanki, S. K., & Montavon, C. A. P. 1993, A&A, 275, 283
Stellmacher, G., & Wiehr, E. 1971, Sol. Phys., 17, 21
Stellmacher, G., & Wiehr, E. 1980, A&A, 82, 157
Thomas, J. H. 1994, in Solar Surface Magnetism, ed. R. J. Rutten, & C. J. Shrijver (Kluwer Academic Publisher), 219
Tritschler, A., Schlichenmaier, R., Bellot Rubio, L., & the KAOS Team 2004, A&A, 415, 717 (Paper I)
Westendorp Plaza, C., del Toro Iniesta, J. C., Ruiz Cobo, B., et al. 1997, Nature, 389, 47
Westendorp Plaza, C., del Toro Iniesta, J. C., Ruiz Cobo, B., & Martínez Pillet, V. 2001a, ApJ, 547, 1148
Westendorp Plaza, C., del Toro Iniesta, J. C., Ruiz Cobo, B., et al. 2001b, ApJ, 547, 1130
Wiehr, E. 1999, in Third Advances in Solar Physics Euroconference: Magnetic Fields and Oscillations, ed. B. Schmieder, A. Hofmann, & J. Staude, ASP Conf. Ser., 184, 86
Wiehr, E., Koch, A., Knölker, M., Küveler, G., & Stellmacher, G. 1984, A&A, 140, 352